Relativistic *B*-spline *R*-matrix method for electron collisions with atoms and ions: Application to low-energy electron scattering from Cs

Oleg Zatsarinny* and Klaus Bartschat†
Department of Physics and Astronomy, Drake University, Des Moines, Iowa 50311, USA
(Received 8 April 2008; published 4 June 2008)

The *B*-spline *R*-matrix method with nonorthogonal orbital sets is extended to a fully relativistic version based on the solution of the many-electron Dirac equation. The *B*-spline basis is used to generate both the target description and the *R*-matrix basis functions in the inner region. Using *B*-splines of different orders for the large and small components prevents the appearance of pseudostates in the spectrum of the Dirac equation. Using term-dependent and thus nonorthogonal sets of one-electron functions enables us to generate accurate and flexible representations of the target states and the scattering function. Our method is based upon the all-electron Dirac-Coulomb Hamiltonian and thus may be employed for any complex atom or ion, without the use of phenomenological core potentials. As a first test of the method, we consider elastic electron scattering from Cs atoms in their ground state. Close agreement with experiment is obtained for the total and the angle differential cross sections at various energies between 1 eV to 7 eV, as well as for several spin asymmetry parameters. The results represent a substantial improvement over those obtained in previous Breit-Pauli and Dirac *R*-matrix calculations.

DOI: 10.1103/PhysRevA.77.062701 PACS number(s): 34.80.Bm, 34.80.Dp

I. INTRODUCTION

Relativistic effects are well known to be crucially important for electron scattering from heavy targets. Consequently, serious efforts have been devoted over the past decades to incorporating these effects in numerical calculations. One such scheme is the widely used Breit-Pauli-based *R*-matrix (close-coupling) approach [1]. Another possibility is to adopt the Dirac equation from the beginning and thus avoid the approximations made otherwise [2]. Note that relativistic effects may be significant in both the target structure and the collision dynamics. A relativistic approach based on the Dirac equation has the advantage that all relativistic effects are included, not only for the energies, but most importantly already in the radial wave functions.

A Dirac scheme was already implemented in the relativistic "Dirac atomic *R*-matrix code" (DARC) developed by Norrington and Grant [3,4]. This code, as well as its nonrelativistic and semirelativistic companion RMATRIX-I [5] is based on the standard implementation developed by Burke and collaborators in Belfast. Although highly successful in many applications of photon and electron collisions with atoms, ions, and molecules (see, for example, Ref. [6]), the method has limitations, especially when used for very complex targets.

Over the past few years, we have developed the alternative *R*-matrix package BSR [7], which addresses some of the difficulties with the established implementation of the method. The two essential refinements are (i) the removal of orthogonality restrictions, which allows for the use of nonorthogonal orbital sets to represent both the bound and continuum one-electron orbitals, and (ii) the use of *B*-splines as a universal and effectively complete basis to generate the *R*-matrix functions. These features often allow us to achieve a high accuracy in the description of the target states, as well as a truly consistent description of the scattering system. The BSR code, in both its nonrelativistic and semirelativistic (Breit-Pauli) forms, was successfully applied to many problems of electron collisions from atoms and ions, including photoionization, photodetachment, and atomic structure calculations. Without giving a full list of references (some can be found in Ref. [7]), highlights include benchmark calculations for low-energy electron scattering from Ne [8], Ar [9], and Fe^+ [10], and the resolution of long-standing discrepancies between experiment and theory for the spin asymmetry function in electron impact excitation of Ar and Kr [11].

However, it has become clear that the present BSR code does not do as well for cases such as *e*-Xe collisions, simply due to the fact that the spin-orbit interaction is becoming too large to treat it at the level of first-order perturbation theory, i.e., calculating relativistic corrections to the energies while using effectively nonrelativistic wave functions [12]. It is therefore desirable to produce a fully relativistic, all-electron version of the BSR code, which retains all the refinements developed in the semirelativistic version.

The present paper reports on our recent development of this method. As a test example, we choose the low-energy *e*-Cs problem. Electron scattering from Cs has received considerable attention over the past three decades, theoretically and experimentally. For this heavy open-shell target, relativistic effects can be expected to be very important, especially for the calculation of angle-differential spin asymmetries measured by Baum *et al.* [13,14]. There are numerous calculations available for this problem, based on approximations covering a wide range of complexity. These include nonrelativistic approaches such as a two-state model employed by Karule [15] to a convergent close-coupling (CCC) method used by Bray [16], several Breit-Pauli *R*-matrix calculations by Bartschat and collaborators [17–19], and fully relativistic calculations using DARC [20], an independent

*oleg.zatsarinny@drake.edu
†klaus.bartschat@drake.edu

 ©2008 The American Physical Society

Dirac R-matrix approach developed by Thumm and Norcross [21,22], and most recently a relativistic convergent close-coupling method (RCCC) developed by Fursa and Bray [23]. In contrast to DARC, the latter two methods treat the Cs atom as a quasi-one-electron target. This has the advantage of being able to improve the target description by adding semiempirical local model potentials to account, for example, for core-polarization and/or exchange effects. However, such an approach is not general, and it is ultimately limited to a few columns of the period system. For completeness, we note that a fully relativistic distorted-wave method was also recently applied to this problem [24].

This paper is organized as follows. After describing the general approach in Sec. II, we illustrate the current application to e-Cs collisions in Sec. III. Results are presented and discussed in Sec. IV, followed by the conclusions and an outlook to future work.

II. GENERAL THEORY

We use the Dirac-Coulomb (DC) Hamiltonian to describe the N-electron target and the $(N+1)$-electron collision systems, respectively. In atomic units, the DC Hamiltonian for N electrons in a central field made by the nucleus of charge Z is given by

$$H^{\mathrm{DC}} = \sum_{i=1}^{N} \left(c\boldsymbol{\alpha}\cdot\boldsymbol{p}_i + \beta c^2 - \frac{Z}{r_i} \right) + \sum_{i>j}^{N} \frac{1}{r_{ij}}, \tag{1}$$

where the components of the vector $\boldsymbol{\alpha}$ and β are the Dirac matrices, $\boldsymbol{p}_i$ is the momentum operator of electron "i," and $c \approx 137$ is the speed of light. For each partial-wave symmetry J^{π}, with J denoting the total electronic angular momentum in a jj-coupling scheme and π indicating the parity, the total wave function is constructed from Dirac four-component spinors

$$\phi_{n\kappa m} = \frac{1}{r} \begin{pmatrix} P_{n\kappa}(r)\chi_{\kappa m}(\vartheta,\varphi) \\ iQ_{n\kappa}(r)\chi_{-\kappa m}(\vartheta,\varphi) \end{pmatrix}, \tag{2}$$

where the real and imaginary radial Pauli spinors are the large and small components, respectively, χ_{km} is the spinor spherical harmonic, and κ is the relativistic angular momentum quantum number.

The theoretical basis of the Dirac R-matrix method was already described more than 30 years ago by Chang [2]. As mentioned previously, a general numerical implementation (DARC), was developed by Norrington and Grant [3,4]. Recent reviews of the method and some applications can be found in Refs. [25,26].

The present work is an entirely independent implementation of the same basic theory, albeit with two distinctive features that have proven to be of significant advantage, especially for the application to truly complex systems. The first of these features concerns the orthogonality requirements for the one-electron radial functions. Although the option is still available, we generally do not impose any orthogonality conditions on the one-electron radial functions used to represent different target states, and the continuum orbitals do not have to be orthogonal to the bound orbitals either. The use of nonorthogonal orbital sets avoids the need to introduce additional $(N+1)$-electron terms in the R-matrix expansion for the continuum electron. Most importantly, however, it makes it possible to optimize, and then to use in the subsequent collision calculation, the radial wave functions independently for each target state. Consequently, the size of otherwise extensive multiconfiguration expansions, often with correlated pseudo-orbitals being employed to improve the target states, can be reduced significantly.

The second feature is the use of B-splines as a numerically convenient, universal, and effectively complete basis to expand the radial orbitals of interest. It turns out, however, that the relativistic implementation of this basis poses new challenges, particular in collision calculations. These will be further discussed below.

In the spirit of the R-matrix method, the configuration space is partitioned into two regions separated by the R-matrix boundary at $r=a$. The latter is chosen in such a way that the magnitude of the radial spinors describing the bound electrons in the target is sufficiently small that exchange between the incident electron and any target electron outside the R-matrix sphere is negligible. In the inner region, the total scattering wave function is expanded in terms of a basis set,

$$\Psi_k^{N+1} = \sum_{ij} c_{ijk}\mathcal{A}[\Psi_i^N, u_{ij}] + \sum_m d_{mk}\Theta_m^{N+1}. \tag{3}$$

Here Ψ_i^N is the wave function of the N-electron target state i while the u_{ij} form the R-matrix basis for the scattering electron. The Θ_m^{N+1} functions, which must be included to compensate for any orthogonality constraints imposed on u_{ij}, are usually avoided in our case, but they can be used under special circumstances. They are $(N+1)$-electron square-integrable functions constructed by adding a valence electron to a target state. The symbol $\mathcal{A}$ represents the angular coupling and antisymmetrization between the incident projectile and the target electrons. The coefficients c_{ijk} and d_{mk} are obtained by diagonalizing the $(N+1)$-electron Dirac-Coulomb Hamiltonian (1).

As mentioned above, a distinctive numerical feature of the present method is the use of B-splines as a universal basis to represent the scattering orbitals in the inner region of $r \le a$. B-splines of order k, defined on a knot sequence $\{t_i, i=1,2,\ldots,n\}$, are piecewise polynomials of degree $k-1$, which can be regarded as a complete basis for continuous functions of class C^{k-2} [27]. Such B-splines were introduced to atomic structure calculations about 20 years ago and became widely used due to their excellent numerical approximation properties. (See, for example, the review by Bachau *et al.* [28].) We implemented B-splines as the R-matrix basis in our semirelativistic R-matrix code BSR [7] and often obtained substantially improved results over previous calculations. The completeness of the B-spline basis is one of the many practical advantages. As a specific example, no Buttle correction to the R-matrix is needed in our implementation. Furthermore, the surface amplitudes that determine the total wave function at the boundary and are required for the evaluation of the R-matrix, are given by the coefficient of the last

spline. This is the only spline with a nonzero value at the boundary.

In contrast to the nonrelativistic case, however, the direct implementation of *B*-splines for the solution of the Dirac equations encounters a problem related to the occurrence of spurious states [29–34]. Fortunately, the wave functions of these states oscillate rapidly, and hence they play a negligible role in the summation over states in many-body perturbation theory (MBPT). For this very reason, these pseudosolutions have been disregarded in practical atomic calculations based on the MBPT [30]. However, since the presence of the spurious states disturbs the spectrum, it worsens the convergence properties of such basis-set calculations [31]. This is of particular concern in *R*-matrix calculations, where one needs the surface amplitudes for each solution. The appearance of these kinds of pseudostates completely destroys the *R*-matrix in the vicinity of such a state.

Several schemes for solving the problem of spurious states have been presented to date. Most recently this problem was investigated in detail by Igarashi [32] who used a variety of methods and boundary conditions. In particular, he explored the use of *B*-splines of different order, k_p and k_q, as a way of avoiding spurious solutions. In a subsequent paper [33], he concluded that "kinetic balance" also provided a good basis. Rather than *B*-splines alone, combinations of the form $B'(r) \pm \kappa B(r)/r$, with the prime denoting the first derivative, are employed instead in this case. The kinetic balance basis, however, and even more so the dual kinetic balance approach proposed in Ref. [31], is very difficult to implement, particularly in multichannel *R*-matrix calculations, since different bases are needed for different values of κ. This makes such a basis impractical for calculations with extensive multiconfigurational expansions.

A practically feasible solution was recently proposed by Froese Fischer and Zatsarinny [34]. They noticed that the (B, B') and the (B^k, B^{k+1}) functions are a numerically very stable basis, thereby avoiding the occurrence of spurious solutions. At the same time, this basis retains the simplicity and effectiveness of the original *B*-spline basis and provides the same accuracy as the kinetic balance bases proposed by Igarashi [33].

Based on these findings, we expand the radial functions for the large and small components $P(r)$ and $Q(r)$ in separate *B*-spline bases as

$$P(r) = \sum_{i=1}^{n_p} p_i B_i^{k_p}(r), \tag{4}$$

$$Q(r) = \sum_{i=1}^{n_q} q_i B_i^{k_q}(r). \tag{5}$$

Both *B*-spline bases are defined on the same grid, with the same number of intervals, n_v. Only in this case the calculations of various matrix elements and integrals of interest can be performed with the same routines and at the same level of required computational resources as in the case of a single *B*-spline basis.

The coefficients p_i and q_i are found by diagonalizing the total $(N+1)$-electron Hamiltonian inside the *R*-matrix box. More specifically, using the *B*-spline basis leads to a generalized eigenvalue problem of the form

$$\boldsymbol{Hc} = E\boldsymbol{Sc}, \tag{6}$$

where $\boldsymbol{S}$ is the overlap matrix between the basis functions. If orthogonality conditions are imposed between the scattering orbitals, $\boldsymbol{S}$ reduces to a banded matrix whose elements are the overlaps between individual *B*-splines. In the general case of nonorthogonal orbital sets, however, it has a more complicated structure. The *R*-matrix basis functions for the continuum electron are chosen to satisfy the boundary conditions [4]

$$\frac{Q_i(a)}{P_i(a)} = \frac{b+\kappa}{2ac} = \mu, \tag{7}$$

where b is an arbitrary constant usually chosen as 0.

With nonzero solutions on the boundary, the interaction matrix $\boldsymbol{H}$ in Eq. (6) becomes non-Hermitian. In *R*-matrix theory, it is customary to apply a Bloch operator that enforces the boundary conditions as well as symmetry. We use the Bloch operator suggested in Ref. [35],

$$\mathcal{L} = c\,\delta(r-a)\begin{pmatrix} -\mu\eta & \eta \\ (\eta-1) & (1-\eta)/\mu, \end{pmatrix}, \tag{8}$$

where μ defines the boundary conditions (7) and η is an arbitrary constant. In the present calculations we used $\eta = 1/2$.

After adding the Bloch operator to the Hamiltonian, the interaction matrix is reduced to symmetric form and can be diagonalized readily to obtain the desired set of solutions. From this finite set of solutions, an *R*-matrix relation can be derived that connects the solutions in the inner and outer regions. For a given energy E, this relation has the form

$$P_i(a) = \sum_j R_{ij}(E)[2acQ_j(a) - (b+\kappa)P_j(a)], \tag{9}$$

where the relativistic *R*-matrix is defined as

$$R_{ij}(E) = \frac{1}{2a}\sum_k \frac{P_{ik}(a)P_{jk}(a)}{E_k^{N+1} - E}. \tag{10}$$

Here the E_k^{N+1} are the *R*-matrix poles while the P_{ik} are the surface amplitudes of Ψ_k in channel i. We note that a more rigorous expression for the *R*-matrix contains the correction $-(b+\kappa)/[(b+\kappa)^2+(2ac)^2]$, first obtained by Szmytkowski and Hinze [35]. This correction is due to the fact that the set of relativistic basis functions (P_i, Q_i) is incomplete on the surface $r=a$. In most realistic cases, however, it is small and thus usually omitted.

The reactance matrix in the *R*-matrix method is defined via the matching of the external and internal solutions at $r=a$. In the external region, exchange between the scattered electron and the target electrons is neglected. Consequently, the channel wave functions satisfy a set of coupled differential equations described in detail in Ref. [36]. Except if the target is very highly charged, the scattered electron can be well described in a nonrelativistic framework. In the

present calculations, therefore, we follow [2,3] and use the nonrelativistic limit of the Dirac radial equations for the scattered electron in the asymptotic region. In this case, the matching procedure is identical to that used in the semirelativistic BSR code [7].

III. APPLICATION: ELECTRON SCATTERING FROM NEUTRAL CS

The Cs atom, in the ground and low excited states, has the relatively simple configurations $[1s^2\cdots 5p^6](nl)^2L$. In most previous calculations, therefore, Cs was modeled as a quasi-one-electron atom with one active electron above the closed Xe-like inert core of a Cs^+ ion. A phenomenological one-electron core polarization potential was usually added to account for the core-valence correlation. Although such a potential simplifies the calculations significantly and can provide accurate excitation energies and oscillator strengths, the question always remains how well the model potential can simulate all core-valence correlation, including nondipole contributions. In the present approach, we therefore choose to include the core-valence correlation *ab initio* by adding target configurations with an excited core. All target states were generated with the *B*-spline box-based close-coupling method described in Ref. [37]. This method also provides a systematic way of constructing pseudostates, which are important for the *e*-Cs collision problem, especially at "intermediate" incident energies from about one to a few times the ionization threshold.

Specifically, the calculation of the target states included the following steps. We started by generating the core orbitals from a Dirac-Fock calculation for Cs^+ and then obtained valence nl orbitals for Cs with the Cs^+ core frozen. Next, the core-valence correlation was simulated by adding the $5s^25p^5\bar{n}\ell\bar{n}\ell'$ and the $5s5p^6\bar{n}\ell\bar{n}\ell'$ configurations, where the bar indicates a correlated rather than a physical orbital. All Dirac-Fock calculations for the core and the correlated orbitals were performed with the GRASP2K relativistic atomic structure package [38]. Different sets of correlated orbitals $\bar{n}\ell$ were optimized separately for the lowest state of each symmetry with target electronic angular momentum $(nl)J^\pi$. Since the mean radii for the $\bar{n}\ell$ orbitals are between the mean radii of the core and the valence orbitals, this method allows us to incorporate the core-valence correlation with a relatively small number of configurations. Then, the entire spectrum of Cs was recalculated using the *B*-spline box-based expansion

$$\begin{aligned}\Phi(5s^25p^6nl;J\pi) = \mathcal{A}[&\varphi(5s_{1/2}^2 5p_{1/2}^2 5p_{3/2}^4)\phi(n\ell)]^{J\pi} \\ &+ a_i\varphi(5s_{1/2}^2 5p_{1/2}^2 5p_{3/2}^3 \bar{n}\ell\bar{n}\ell';J\pi) \\ &+ b_i\varphi(5s_{1/2}^2 5p_{1/2}^1 5p_{3/2}^4 \bar{n}\ell\bar{n}\ell';J\pi) \\ &+ c_i\varphi(5s_{1/2} 5p_{1/2}^2 5p_{3/2}^4 \bar{n}\ell\bar{n}\ell';J\pi),\end{aligned} \tag{11}$$

where $\mathcal{A}$ again denotes the antisymmetrization operator. The unknown large and small radial components for the outer valence electron, $\phi(n\ell)$, were expanded in the *B*-spline basis as shown in Eqs. (4) and (5). The coefficients of the *B*-spline expansions, p_i and q_i, together with the coefficients for the correlated configurations, a_i, b_i, and c_i, were found by diagonalizing the Dirac-Coulomb Hamiltonian (1) with the additional requirement that the wave functions vanish at the boundary. Note that we do not impose orthogonality of the valence orbitals $n\ell$ to the correlated orbitals $\bar{n}\ell$ in the above procedure. This speeds up the convergence of the expansion (11) and yields accurate binding energies with a relatively small number ($\sim$50) of correlated configurations for each symmetry.

The number of physical states that we can generate in this method depends upon the size a of the *R*-matrix box. We chose $a=50\,a_0$, which allowed us to obtain a good description for all low-lying bound states of Cs up to 9*s*. Along with these physical states, we also generated a set of pseudostates for each symmetry, with the lowest states representing the remaining bound states and the others representing the continuum. Note that the resulting pseudostates also contain the core-excited states with configurations $5s^25p^5n\ell n\ell'$ and $5s5p^6n\ell n\ell'$, which lie in the Cs continuum spectrum.

In the present calculations we included 110 *B*-splines of order 8 for the large component and 111 *B*-splines of order 9 for the small component. The different *B*-spline orders for the two components guarantee the absence of spurious solutions in the generated Cs spectrum [34]. We used a semiexponential grid for the *B*-spline knot sequence. The relatively large number of splines is due to the fact that we employed a finite-size nuclear model with a Fermi potential. In order to correctly describe this potential near the nucleus, we needed to define a very fine knot sequence at small *r*, with the first nonzero knot at $r_1=10^{-8}$. The resulting excitation energies of the target states agree with experiment within 10 meV for all states up to $(5f)^F_{5/2,7/2}$.

The number of *B*-splines and the *R*-matrix radius in the scattering calculations were chosen the same as in the calculation of the target bound states. Our main scattering model (12CC) contains 12 target states, namely the six bound states $(6s)^2S_{1/2}$, $(6p)^2P_{1/2,3/2}$, $(5d)^2D_{3/2,5/2}$, and $(7s)^2S_{1/2}$ of Cs together with six pseudostates. The latter were selected from the entire spectrum based on the strongest dipole connection to the ground state. We numerically calculated partial-wave contributions up to $J=50$. The calculations of the cross section and all other scattering parameters of interest were then carried out in the same way as in standard *R*-matrix treatments. In order to check the convergence of the close-coupling expansion, we also performed calculations with two extended scattering models for low partial ways up to $J=15$. Specifically, these were a 20-state (20CC) model, including only bound states but going up to $(5f)^2F_{5/2,7/2}$, and a 30-state (30CC) model that added another 10 pseudostates lying in the continuum.

IV. RESULTS AND DISCUSSION

Figure 1 compares our predicted total cross section for electron collisions with Cs in its $(6s)^2S_{1/2}$ ground state with several experimental data sets and some recent theoretical results. We see close agreement of our results with the absolute experimental data over a wide range of incident energies

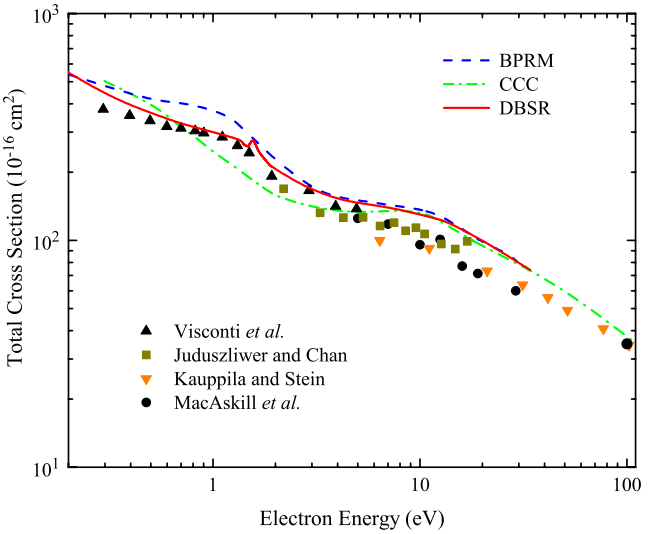

FIG. 1. (Color online) Total electron scattering cross section from the $(6s)^2S$ ground state of Cs. The present 12-state DBSR results are compared with various sets of experimental data [39–42], as well as predictions from a 40-state semirelativistic Breit-Pauli *R*-matrix calculation [19] (BPRM) and a nonrelativistic CCC model [42].

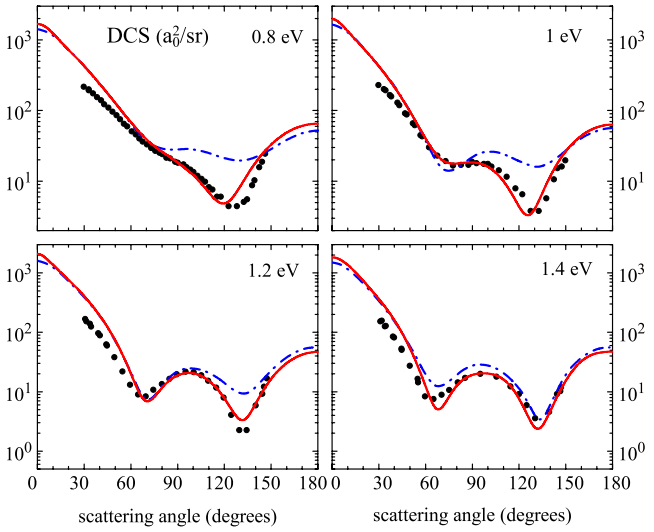

FIG. 2. (Color online) Angle differential cross section for elastic *e*-Cs collisions at 0.8, 1.0, 1.2, and 1.4 eV. The relative experimental data of Gehenn and Reichert [43] (•) were normalized to the present 12-state DBSR results (solid line) at the scattering angle of 90°. Also shown are the fully relativistic five-state *R*-matrix results of Thumm and Norcross [22] (dashed-dotted line).

between 0.5 eV to 100 eV. For energies above 10 eV, all the theoretical results displayed are very close to each other, but they slightly exceed the experimental values. For energies above 100 eV (not shown in the figure), there is very close agreement between experiment and theoretical predictions from a nonrelativistic CCC model [42]. Hence, cross sections in this region can be considered as having been reliably established. However, there are noticeable discrepancies at energies below 10 eV. Our results seem to agree somewhat better with the experimental data of Visconti *et al.* [39] than those obtained in the 40-state semirelativistic Breit-Pauli *R*-matrix (BPRM) or the nonrelativistic CCC method, especially regarding the energy dependence of the total cross section. However, there is only one set of experimental data available in this energy regime, and hence it seems premature to draw definite conclusions. It would be highly desirable to have additional experimental data, as well as RCCC predictions.

The discrepancies between the CCC and the Breit-Pauli results are most likely due to structure differences. Note that structure approximations for the target states can become equally important to those made in a collision model. Both the CCC and the Breit-Pauli calculations used a frozen Hartree-Fock core together with phenomenological one-electron and two-electron core polarization potentials to describe the valence and the projectile electrons. On the other hand, we employed extensive CI expansions with open-core configurations in the present calculations. These allow for an *ab initio* description of core-polarization effects, including nondipole contributions. We found a fast convergence of the results for the total cross section with respect to the number of target states included in the close-coupling expansion, with differences between the 12CC, 20CC, and 30CC results of about 1%–2%. This is not unexpected, since the total cross section is the angle-integrated sum of elastic, excitation, and ionization cross sections. It is likely one of the least sensitive parameters to the details of a collision model.

Angle differential cross sections (DCS), on the other hand, provide a more rigorous test for scattering calculations. Figure 2 shows the DCS for energies around 1 eV. In this energy range, a previous fully relativistic Dirac *R*-matrix calculation by Thumm and Norcross [22] did not reproduce the experimental angular dependence, particularly regarding the minima for scattering angles around 130° at incident energies of 0.8, 1.0, and 1.2 eV. In the various panels, the relative experimental data of Gehenn and Reichert [43] were normalized to our results at $\theta \approx 90°$. Except for the minima mentioned above, which our results exhibit in excellent accordance with experiment, the agreement between the two sets of theoretical results is good. We suspect that the remaining discrepancies are once again due to differences in the structure model, and they are more likely to show up when the numbers are small. Note that Thumm and Norcross also modeled the *e*-Cs collision complex as a quasi-two-electron system, where two active electrons (the scattered electron and the valence electron of the target) interact with the target core through semiempirical Thomas-Fermi-type and core-polarization potentials. Interestingly, a nonrelativistic two-state close-coupling calculation by Karule [15] (not shown) also agreed very well with experiment at these low energies. This agreement, however, seems somewhat fortuitous, since there are significant deviations between Karule's predictions and experiment for energies around 2 eV and higher. For the latter energies, both the present calculations and those of Ref. [22] show very close agreement with each other and also with experiment.

An even more detailed test of theory is provided by various spin-asymmetry parameters that describe the scattering of (possibly) spin-polarized electrons from (possibly) spin-polarized atoms. For elastic *e*-Cs collisions, results from

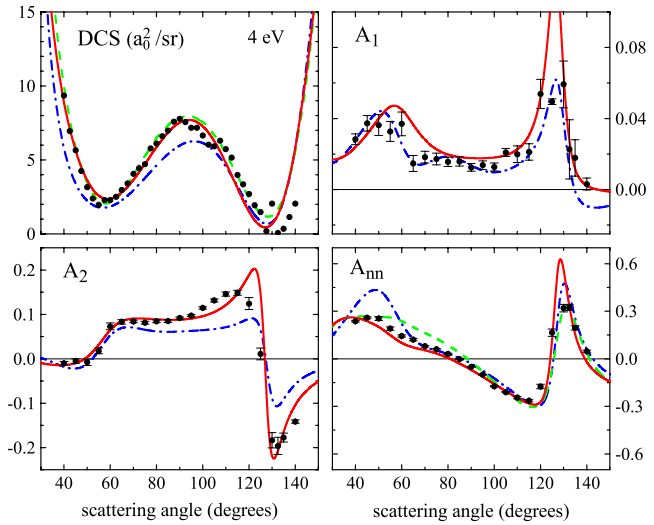

FIG. 3. (Color online) Angle differential cross section and asymmetry parameters for elastic electron scattering from Cs at 4 eV. The experimental data of Baum *et al.* [14] (•) are compared with the present 12-state DBSR results (solid line) and those from a semirelativistic BPRM [14] (dashed-dotted line) and a nonrelativistic CCC calculation [16] (dashed line).

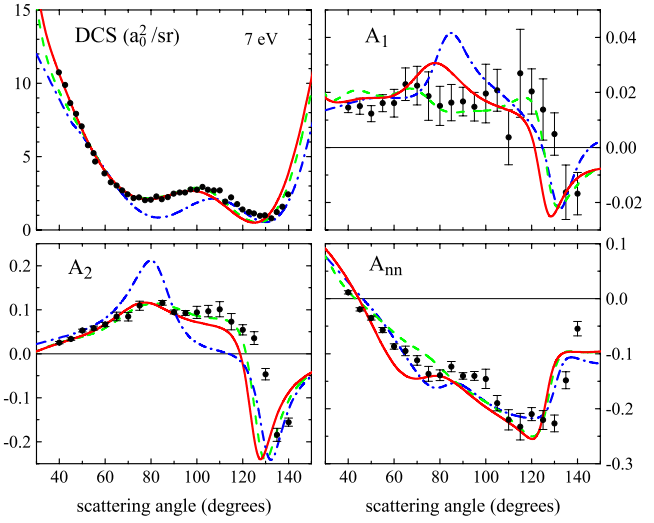

FIG. 4. (Color online) Angle differential cross section and asymmetry parameters for elastic electron scattering from Cs at 7 eV. The experimental data of Baum *et al.* [14] (•) are compared with the present 30-state DBSR results (solid line) and those from a semirelativistic BPRM [14] (dashed-dotted line) and a fully relativistic RCCC calculation [23] (dashed line).

such experiments were reported by Baum *et al.* [13,14]. Along with the relative DCS for incident energies from 3 eV to 25 eV, they measured the set of spin-asymmetry parameters A_1, A_2, and A_{nn}. These describe, respectively, the left-right asymmetry in the scattering of an initially unpolarized electron beam after scattering from a polarized target with polarization vector perpendicular to the scattering plane (A_1), a similar left-right asymmetry if the incident electron beam is polarized (again perpendicular to the scattering plane) but the target is unpolarized (A_2), and finally the angle-resolved asymmetry in the scattering intensity for antiparallel vs parallel orientations of both the electron and the target polarizations (A_{nn}). As noted by Farago [44], A_{nn} is most sensitive to electron exchange effects and can already be nonzero in a nonrelativistic model of e-Cs collisions. On the other hand, A_2 requires the spin-orbit interaction for the projectile electron, while A_1 requires both the spin-orbit interaction and electron exchange to be important. Consequently, any nonrelativistic collision model, such as the CCC calculations reported in Ref. [16], will yield exactly zero for both A_1 and A_2. Interestingly, the latter model produced excellent results for the DCS and A_{nn} at the same time. This is mostly due to the cancellation of small differences in the various partial cross sections that make up these asymmetries [19].

Figure 3 exhibits our results for 4 eV and compares them with experiment as well as BPRM [19] and (for the DCS and A_{nn} only) nonrelativistic CCC [16] predictions. The 12-state DBSR results agree better with the CCC than the BPRM numbers and reproduce the angular dependence of all experimental data in a very satisfactory way. We note that a recent relativistic distorted-wave calculation by Ahmed *et al.* [24] also yielded good agreement for the A_2 parameter and the angular dependence of the DCS for a number of energies. However, the absolute DCS values often differed significantly from the present DBSR and the CCC results. Unfortunately, no RDW results for A_1 and A_{nn}, nor for the total cross section, were presented.

As mentioned above, Fursa and Bray [23] recently reported the development of the fully relativistic RCCC method. They also used elastic electron scattering from the ground state of cesium, this time at the single collision energy of 7 eV, to demonstrate the capability of their approach. This is a particularly difficult collision energy for theory (about twice times the ionization threshold), at which coupling effects to the continuum are likely to be most important. Figure 4 shows results at this energy. We note excellent agreement between the present DBSR and the RCCC results for the DCS as well as the "relativistic" spin asymmetries A_1 and A_2, and there is also very satisfactory agreement with the experimental data of Baum *et al.* [14]. There seems to be a small shift of about $5°-10°$ in the second minimum of the DCS around 135° and, consequently, the angular range over which the spin asymmetries vary substantially. Both of these models represent a significant improvement over the BPRM calculations for these parameters.

Interestingly, the situation is slightly different for the "exchange asymmetry" A_{nn}, where the RCCC and the BPRM calculations show very good agreement with experiment while the DBSR results lie somewhat below the experimental data in the angular range from 50° to 70°. We performed extensive checks to track down the origin of this relatively small discrepancy and found a very slow convergence for the A_{nn} parameter with the number of states in the close-coupling expansion. The 12-state results differed significantly from the 30-state DBSR results shown in Fig. 4. This is the biggest calculation that could be performed with our currently available computational resources. These findings indicate the importance of channel coupling at this particular energy.

V. SUMMARY AND OUTLOOK

In this paper, we have introduced a Dirac-based version of the *B*-spline *R*-matrix method. The present DBSR approach retains all the advantages of the previous semirelativistic version, including its generality as an all-electron code and the flexibility associated with the use of nonorthogonal orbital sets. Not only valence and core-valence correlations, but also relativistic effects are now treated *ab initio* by employing the many-electron Dirac-Coulomb Hamiltonian.

Our first test case, elastic electron collisions from Cs atoms, revealed good qualitative agreement with previous results obtained in less sophisticated approximations. When differences occurred in the details, substantial improvement in the agreement between theory and experiment was generally achieved. The present results also agree very well with those generated recently in a fully relativistic convergence close-coupling approach [23], thereby providing an independent consistency check for the two methods and the expected assurance that core-valence correlations can be approximated well by a core-potential approach for this particular collision system.

For electron energies above the ionization threshold, the present calculations reveal a slow convergence, both for angle differential cross sections and asymmetry parameters. In order to achieve convergence with the number of states included in the close-coupling expansion, we should ideally include all pseudostates with energies below and even slightly above the collision energies of interest. This will require the diagonalization of large interaction matrixes, whose rank could quickly exceed 50 000 and will make it impractical to run the code on serial machines. In addition to further additional tests on more complex systems such as Xe, Au, and Hg, parallelization of the DBSR complex will therefore be the next major step in our development of the package.

ACKNOWLEDGMENTS

We would like to thank Dmitry Fursa for sending the RCCC results in numerical form. This work was supported by the United States National Science Foundation under Grants No. PHY-0244470, No. PHY-0555226, and No. PHY-0757755.

[1] N. S. Scott and P. G. Burke, J. Phys. B **13**, 4299 (1980).
[2] J. J. Chang, J. Phys. B **8**, 2327 (1975); **10**, 3335 (1977).
[3] P. H. Norrington and I. P. Grant, J. Phys. B **14**, L261 (1981).
[4] P. H. Norrington and I. P. Grant, J. Phys. B **20**, 4869 (1987).
[5] K. A. Berrington, W. B. Eissner, and P. N. Norrington, Comput. Phys. Commun. **41**, 75 (1995).
[6] P. G. Burke and K. A. Berrington, *Atomic and Molecular Processes: An R-Matrix Approach* (Institute of Physics, Bristol, 1993).
[7] O. Zatsarinny, Comput. Phys. Commun. **174**, 273 (2006).
[8] O. Zatsarinny and K. Bartschat, J. Phys. B **37**, 2173 (2004).
[9] O. Zatsarinny and K. Bartschat, J. Phys. B **37**, 4693 (2004).
[10] O. Zatsarinny and K. Bartschat, Phys. Rev. A **72**, 020702(R) (2005).
[11] K. Bartschat and O. Zatsarinny, J. Phys. B **40**, F43 (2007).
[12] M. Allan, O. Zatsarinny, and K. Bartschat, Phys. Rev. A **74**, 030701(R) (2006).
[13] G. Baum, W. Raith, B. Roth, M. Tondera, K. Bartschat, I. Bray, S. Ait-Tahar, I. P. Grant, and P. H. Norrington, Phys. Rev. Lett. **82**, 1128 (1999).
[14] G. Baum, N. Pavlovic, B. Roth, K. Bartschat, Y. Fang, and I. Bray, Phys. Rev. A **66**, 022705 (2002).
[15] E. Karule, J. Phys. B **5**, 2051 (1972).
[16] K. Bartschat and I. Bray, Phys. Rev. A **54**, 1723 (1996).
[17] N. S. Scott, K. Bartschat, P. G. Burke, W. B. Eissner, and O. Nagy, J. Phys. B **17**, L191 (1984).
[18] K. Bartschat, J. Phys. B **26**, 3595 (1993).
[19] T. Kirchner, M. Horbatsch, and H. J. Ludde, Phys. Rev. A **66**, 052719 (2002).
[20] S. Ait-Tahar, I. P. Grant, and P. H. Norrington, Phys. Rev. Lett. **79**, 2955 (1997).
[21] U. Thumm and D. W. Norcross, Phys. Rev. Lett. **67**, 3495 (1991).
[22] U. Thumm and D. W. Norcross, Phys. Rev. A **47**, 305 (1993).
[23] D. V. Fursa and I. Bray, Phys. Rev. Lett. **100**, 113201 (2008).
[24] Md. F. Ahmed, W. Ji, R. P. McEachran, and A. D. Stauffer, J. Phys. B **40**, 4119 (2007).
[25] I. P. Grant, *Relativistic Quantum Theory of Atoms and Molecules* (Springer, New York, 2007).
[26] I. P. Grant, J. Phys. B **41**, 055002 (2008).
[27] C. de Boor, *A Practical Guide to Splines* (Springer, New York, 1978).
[28] H. Bachau, E. Cormier, P. Decleva, J. E. Hansen, and F. Martin, Rep. Prog. Phys. **64**, 1815 (2001).
[29] W. R. Johnson, S. A. Blundell, and J. Sapirstein, Phys. Rev. A **37**, 307 (1988).
[30] J. Sapirstein and W. R. Johnson, J. Phys. B **29**, 5213 (1996).
[31] V. M. Shabaev, I. I. Tupitsyn, V. A. Yerokhin, G. Plunien, and G. Soff, Phys. Rev. Lett. **93**, 130405 (2004).
[32] A. Igarashi, J. Phys. Soc. Jpn. **75**, 114301 (2006).
[33] A. Igarashi, J. Phys. Soc. Jpn. **76**, 054301 (2007).
[34] C. Froese Fischer and O. Zatsarinny (unpublished).
[35] R. Szmytkowski and J. Hinze, J. Phys. B **29**, 761 (1996).
[36] I. G. Young and P. H. Norrington, Comput. Phys. Commun. **83**, 215 (1994).
[37] O. Zatsarinny and C. Froese Fischer, J. Phys. B **35**, 4669 (2002).
[38] P. Jönsson, X. He, C. Froese Fischer, and I. P. Grant, Comput. Phys. Commun. **177**, 597 (2007).
[39] P. Visconti, J. Slevin, and K. Rubin, Phys. Rev. A **3**, 1310 (1971).
[40] B. Jaduszliwer and Y. C. Chan, Phys. Rev. A **45**, 197 (1992).
[41] T. S. Stein and W. E. Kauppila (unpublished).
[42] J. A. MacAskill, W. Kedzierski, J. W. McConkey, J. Domyslawska, and I. Bray, J. Electron Spectrosc. Relat. Phenom. **123**, 173 (2002); private communication.
[43] W. Gehenn and E. Reichert, J. Phys. B **10**, 3105 (1977).
[44] P. S. Farago, J. Phys. B **7**, L28 (1974).